Hemolytic anemia repressed hepcidin level without hepatocyte iron overload: lesson from Günther disease model

Sarah Millot,[1,2,3,4*] Constance Delaby,[1,3,5*] Boualem Moulouel,[1,3,4]
Thibaud Lefebvre,[1,3,4,6] Nathalie Pilard,[1,3] Nicolas Ducrot,[1,3,4] Cécile Ged,[7]
Philippe Lettéron,[1,3] Lucia de Franceschi,[8] Jean Charles Deybach,[1,3,4,5]
Carole Beaumont,[1,3,4] Laurent Gouya,[1,3,4,6] Hubert De Verneuil,[6]
Saïd Lyoumi,[1,4,9] Hervé Puy[1,3,4,6] and Zoubida Karim[1,3,4]

[1]INSERM U1149/ERL CNRS 8252, Centre de Recherche sur l'Inflammation Paris Montmartre, 75018 Paris, France; [2]Assistance Publique–Hôpitaux de Paris (AP-HP), Service Odontologie, Hôpital Universitaire, Université de Montpellier, France; [3]Université Paris Diderot, Bichat site, Paris, France; [4]Laboratory of Excellence, GR-Ex, Paris, France; [5]Institut de Médecine Régénératrice et de Biothérapie-Hôpital Saint Eloi CHU Montpellier, Université de Montpellier, France; [6]Assistance Publique–Hôpitaux de Paris (AP-HP), Centre Français des Porphyries, Hôpital Louis Mourier, Colombes, France; [7]INSERM, Biothérapies des Maladies Génétiques et Cancers, U1035, F-33000 Bordeaux, France; [8]Department of Clinical and Experimental Medicine, Section of Internal Medicine, University of Verona, Italy and [9]Université Versailles Saint Quentin en Yvelines, France

*SM, CD, HP and ZK contributed equally to this work

ABSTRACT

Hemolysis occurring in hematologic diseases is often associated with an iron loading anemia. This iron overload is the result of a massive outflow of hemoglobin into the bloodstream, but the mechanism of hemoglobin handling has not been fully elucidated. Here, in a congenital erythropoietic porphyria mouse model, we evaluate the impact of hemolysis and regenerative anemia on hepcidin synthesis and iron metabolism. Hemolysis was confirmed by a complete drop in haptoglobin, hemopexin and increased plasma lactate dehydrogenase, an increased red blood cell distribution width and osmotic fragility, a reduced half-life of red blood cells, and increased expression of heme oxygenase 1. The erythropoiesis-induced Fam132b was increased, hepcidin mRNA repressed, and transepithelial iron transport in isolated duodenal loops increased. Iron was mostly accumulated in liver and spleen macrophages but transferrin saturation remained within the normal range. The expression levels of hemoglobin-haptoglobin receptor CD163 and hemopexin receptor CD91 were drastically reduced in both liver and spleen, resulting in heme- and hemoglobin-derived iron elimination in urine. In the kidney, the megalin/cubilin endocytic complex, heme oxygenase 1 and the iron exporter ferroportin were induced, which is reminiscent of significant renal handling of hemoglobin-derived iron. Our results highlight ironbound hemoglobin urinary clearance mechanism and strongly suggest that, in addition to the sequestration of iron in macrophages, kidney may play a major role in protecting hepatocytes from iron overload in chronic hemolysis.

Introduction

Iron homeostasis relies on its storage and recycling through tissue macrophages, which contain the largest iron pool [derived from phagocytosis of senescent red cells and subsequent catabolism of hemoglobin (Hb) and heme]. Such recycling provides most of the daily iron requirement (20-30 mg). However, the intestine also takes part in iron homeostasis by providing 1-2 mg of iron per day, which corre-

sponds to the daily loss of the metal. The major regulator of iron homeostasis is hepcidin (reviewed by Ganz[1]), which is directly down-regulated by stimulated activity of erythropoiesis.[2] Fam132b [Erythroferrone (ERFE)] has been proposed as a crucial cytokine produced by late erythroblast to repress hepcidin synthesis.[3] Since low hepcidin levels favor intestinal iron absorption and mobilization of tissue iron stores, its repression accounts for the paradoxical condition known as iron loading anemia.[4,5] In hemolytic anemia, much less is known about hepcidin expression and the pattern of iron loading compared to anemia with ineffective erythropoiesis. Intravascular hemolysis leads to massive red blood cell (RBC)-free Hb and heme, which are chaperoned by haptoglobin (Hp) and hemopexin (Hpx), respectively, and cleared by spleen and liver macrophages *via* CD163 and CD91, respectively.[6] Subsequent cellular endocytosis of these complexes followed by heme oxygenase 1 (HO-1) pathway activation results in heme catabolism and progressive tissue iron accumulation.

We generated a mouse model of congenital erythropoietic porphyria (CEP; MIM 2637007), presenting with chronic hemolysis, to study iron and heme metabolisms and hepcidin expression. CEP or Günther's disease is a rare autosomal recessive disorder[8] caused by partial deficiency of Uroporphyrinogen III Synthase (UROS; EC 4.2.1.75), the fourth enzyme of heme metabolism. This deficiency leads to excessive synthesis and accumulation of pathogenic type I isomers of hydrophilic porphyrins (uroporphyrin I and coproporphyrin I) in bone marrow erythroid cells, leading to intravascular hemolysis with massive appearance of these compounds in plasma and urine.[9] CEP patients suffer from chronic hemolysis without symptoms of ineffective erythropoiesis[10] and from cutaneous photosensitivity with mutilating involvement. Clinical severity of anemia is highly heterogeneous among the patients, suggesting a role of modifier genes in the expression of the disease. Indeed, we identified a gain-of-function mutation in ALAS2, the erythroid isoform of the first enzyme of the heme biosynthetic pathway, in a CEP patient with severe hemolytic phenotype.[11] Nevertheless, pathogenesis of hemolysis and iron disturbances resulting from such a chronic hemolysis without an ineffective erythropoiesis model has not yet been characterized.

This study aims to identify the precise pathogenesis of iron disturbance occurring in a chronic hemolysis CEP mouse model. We compared this model to *Hjv*^{−/−} hemochromatosis mice, which exhibited high non-heme iron overload without hemolysis or ineffective erythropoiesis. Our results clearly show that iron metabolism is highly adapted to satisfy the iron needs of bone marrow and spleen for effective erythropoiesis. Hepcidin levels are fully reduced in CEP mice by the regenerative erythropoiesis but do not lead to hepatocyte iron overload. Tissue iron overload derived from heme/Hb is primarily localized in the liver and spleen macrophages rather than hepatocytes. The absence of hepatocyte iron overload is a consequence of both the huge increase in erythroblast production and urinary iron losses. Finally, a tight co-ordination of heme/Hb and iron handling by the liver and kidney, through a dissociation in the tissue expression CD91 and CD163 expression levels limit the toxicity of Hb, heme and iron and allow the recovery of iron needed for erythropoiesis.

Methods

Animals and biochemical analyses

The CEP mouse model was established by knock-in of the human P248Q mutation into the *Uros* gene and subsequently back-crossed on the BALB/c background.[7,12] The hemojuvelin knock-out animals (Hjv-/-) were a kind gift from Nancy Andrews (Duke University, USA). For acute hemolysis and heme-arginate experiments, BALB/c mice were provided by the Janvier laboratory (Janvier, Le Genest Saint Isle, France). Since in male mice the expression of hepcidin has been shown to be repressed by testosterone,[13] our experiments were performed on 12- to 14-week-old female mice, unless mentioned otherwise. For hematologic and biochemical analysis, mice were anesthetized by intraperitoneal (i.p.) injection of a xylazine/ketamine mixture before blood puncture in the orbital sinus on heparin- or EDTA-coated tubes. All experimental procedures involving animals were performed with the approval of the Ethics Committee and in compliance with the French and European regulations on Animal Welfare and Public Health Service. Further details are available in the *Online Supplementary Appendix*.

Cell preparation, RBC turnover and flow cytometry analysis

Spleen cells were isolated by mechanical dissociation using a 70 μm cell strainer in the presence of PBS/EDTA/BSA (2 mM/0.5%). Bone marrow cells from femurs and tibias were collected by gentle passage through an 18-gauge needle. Following centrifugation, the cell pellet was washed and resuspended in DMEM (containing 2% FBS and 1 mM HEPES) before flow cytometry analysis. RBC lifespan was assayed by *in vivo* biotinylation followed by FACS analyses, as previously described.[14] Further details are available in the *Online Supplementary Appendix*.

Iron transport studies in duodenal loop

The mice were sacrificed and a segment of approximately 3 cm of duodenum was rapidly isolated and immersed in cold HBSS pH 7.5. Iron transport was monitored by filling the duodenal segment with 100 μL/cm of the radiolabeled transport solution and placing it in a normal HBSS warm bath with 95% O_2 / 5% CO_2 gas as previously described.[15] Then, aliquots from the bath were taken every 5 min for 55Fe-counting by liquid scintillation. Iron transport activity was evaluated as a ratio of counts per duodenum length (cm).

Porphyrin assay, glucose-6-phosphate dehydrogenase activity and erythropoietin assay

Porphyrins were extracted and analyzed by high performance liquid chromatography (HPLC).[16,17] Glucose-6-phosphate dehydrogenase (G6PD) activity was determined using RANDOX G6PDH kit (RANDOX Laboratories Ltd., Antrim, UK). Serum concentration of erythropoietin (epo) was determined using an assay kit (R&D Systems).

Western blot analysis

Crude membrane fractions from mouse tissues were prepared as previously described.[18,19] Briefly, 10-20 μg of crude membrane proteins were solubilized in 1× Laemmli buffer, analyzed by SDS/PAGE and transferred onto a PVDF membrane for HO-1, ferroportin, TfR1, H-ferritin and DMT1. For Hpx detection, 1 μL of plasma was loaded on SDS/PAGE and transferred onto nitrocellulose membrane. Primary antibodies used were: anti-ferroportin (a kind gift from D. Haile, San Antonio, USA), anti-H ferritin (kindly provided by Dr P. Arosio, Brescia, Italy), anti-HO1 (Stressgen Biotechnologies), anti-DMT1 (kindly provided by Dr B. Galy, Heidelberg, Germany), anti-cubilin and anti-megalin (kindly pro-

vided by Dr R. Nielsen, Aarhus, Denmark), anti-β-actin (Sigma, Saint Quentin Fallavier, France), and anti-Hpx (kindly provided by Dr E. Tolosano, University of Torino, Italy). The blots were revealed by ECL® (GE Healthcare) after secondary antibody incubations.

Quantitative RT-PCR

Total RNA from tissue was isolated using an RNA Plus Extraction Solution, as previously described.[20] The results were arbitrarily normalized using the sample with the lowest C_T value for S14, actin or GAPDH, as indicated. The relative quantifications were calculated using the comparative CT method. The amplification efficiency of each target was determined using serial 2-fold dilutions of cDNA. Sequences of the primers are available in the *Online Supplementary Appendix.*

Statistical analysis

For biochemical and hematologic parameters, statistical significance was evaluated using the two-tailed Student *t*-test for comparison between means of two unpaired groups. Two-way ANOVA was used to compare the area under the curves for the duodenal loop experiments. GraphPad Prism software (GraphPad Software, San Diego, CA, USA) was used for statistical analysis.

Results

Clinical features of CEP mice

Homozygous CEP mice showed growth retardation, reduced fertility in adults of both sexes, and red-colored serum and urine.[7] Type I porphyrins (Uro and Copro) were increased in urine and feces (*data not shown*) and in RBCs of CEP mice (Table 1). Cyanosis was visible on ears and tails of the young CEP mice but no spontaneous photosensitivity lesion was observed under our husbandry conditions.

Severe hemolytic anemia and reduced RBC half-life in CEP mice

Congenital erythropoietic porphyria mice showed increased serum bilirubin and LDH levels (Table 1), with almost undetectable levels of Hp and Hpx (Figure 1A and B, respectively), which was strongly indicative of hemolytic anemia. Blood smears revealed anisocytosis and poikilocytosis (Figure 1C). The anemia in CEP mice was severe with significant reduction of Hb levels and RBC number (Table 1), regenerative with marked reticulocytosis (28.8±4.2%) (Table 1), and microcytic and hypochromic with reduced mean cell Hb content (9.95±0.64 pg in CEP *vs.* 14.5±0.18 in WT mice) (Table 1). The density distribution of red cells indicated the presence of both dense erythrocytes with mean cell hemoglobin concentration (MCHC) more than 37 g/dL and overhydrated cells with MCHC less than 22 g/dL (Figure 1D). The increased RBC distribution width (RDW) was in agreement with the variation in red cell size in CEP, related to the presence of increased reticulocytes and a subpopulation of microcytic cells (Table 1). The reticulocyte CHr and microcytic reticulocytes (MCVr) were diminished in CEP mice (Table 1), which strongly suggests an early onset of iron deficiency during erythropoietic differentiation.[21]

To further ascertain the hemolytic nature of the anemia, we measured the lifespan of the erythrocytes and revealed that RBC half-life was reduced from 15 days in WT to less than seven days in CEP mice (Figure 1E). However, osmot-

Table 1. Biological and hematologic parameters.

| Parameters	WT (n=6)	CEP (n=6)
RBCs		
Uro I (μmol/L packed RBCs)	2.44±0.37	794±59*
G6PD(IU/g Hb)	22±0.5	47±2
Mature RBCs		
RBCs (x10¹²/L)	10.2±0.3	7.3±0.3*
Hb (g/dL)	14.8±0.9	8.6±0.5*
Hct (%)	43.2±1.6	32.4±0.7*
MCV (fL)	50.9±0.5	34.4±1.6*
MCHC (g/dL)	28.7±0.75	29.7±0.4
CH (pg)	14.5±0.2	9.95±0.64*
RDW (%)	13.7±0.3	32.2±0.6*
Reticulocytes		
Reticulocytes (%)	2.3±0.4	28.8±4.2*
MCVr (fL)	53.4±0.6	44.8±2.4*
MCHCr (g/dL)	26.8±0.7	25.8±0.20
CHr (pg)	14.1±0.2	11.5±0.6*
Serum		
Bilirubin (μmol/L)	5.97±1.34	15.1±3.4*
LDH (UI/L)	889±207	2324±775*
Erythropoietin (ng/L)	156±41	1277±518*
Iron (μmol/L)	38.3±6.5	65±0.7*
Transferrin (g/L)	3.1±0.3	4.5±0.6*

WT: wild-type (controls); CEP: congenital erythropoietic porphyria; RBC: red blood cells; G6PD: glucose-6-phosphate dehydrogenase; Hb: hemoglobin; Hct: hematocrit; MCV: mean corpuscular volume; MCHC: mean cell hemoglobin concentration; CH: hemoglobin content; RDW: RBC distribution width; MCVr: microcytic reticulocytes; MCHCr: reticulocyte mean corpuscular hemoglobin concentration; CHr: reticulocyte hemoglobin content; LDH: lactate dehydrogenase. *$P<0.0025$, two-tailed Student *t*-test. Results are expressed as mean±SD.

ic fragility measurements revealed a higher resistance to lysis of CEP erythrocytes (as compared to WT) in the higher range of NaCl concentrations. Indeed, at NaCl concentration between 5.5 g/L and 9 g/L, 20%-30% more WT erythrocytes were hemolyzed than CEP erythrocytes (Figure 1F). These data suggest that erythrocytes surviving in the circulation are more resistant to *in vitro* hemolysis: they are likely to correspond to reticulocytes and could explain the increased G6PD activity in CEP erythrocytes (Table 1).

Decreased apoptosis of immature erythroblasts and induction of spleen stress erythropoiesis in CEP mice

In mice, bone marrow erythropoiesis is primarily homeostatic whereas "stress erythropoiesis" develops rapidly in the spleen following acute anemia. We analyzed the respective contribution of bone marrow and spleen erythropoiesis in compensating the hemolytic anemia in CEP mice (Figure 2). Using a flow cytometry assay based on cell surface expression of Ter119 and CD71, as previously described,[14] we visualized larger Ter119⁺CD71⁺ cells [basophilic immature erythroblasts (Ery A)], smaller Ter119⁺CD71⁺cells [polychromatic intermediate erythroblasts (Ery B)] and Ter119⁺CD71⁻ cells [acidophilic late erythroblasts and reticulocytes (Ery C)].

The bone marrow of CEP mice showed an important increase in the number of early erythroblasts (Figure 2A) accompanied by decreased apoptosis (Figure 2B). A moderate but significant increase in intermediate erythroblasts and a decrease in late erythroblasts were also observed
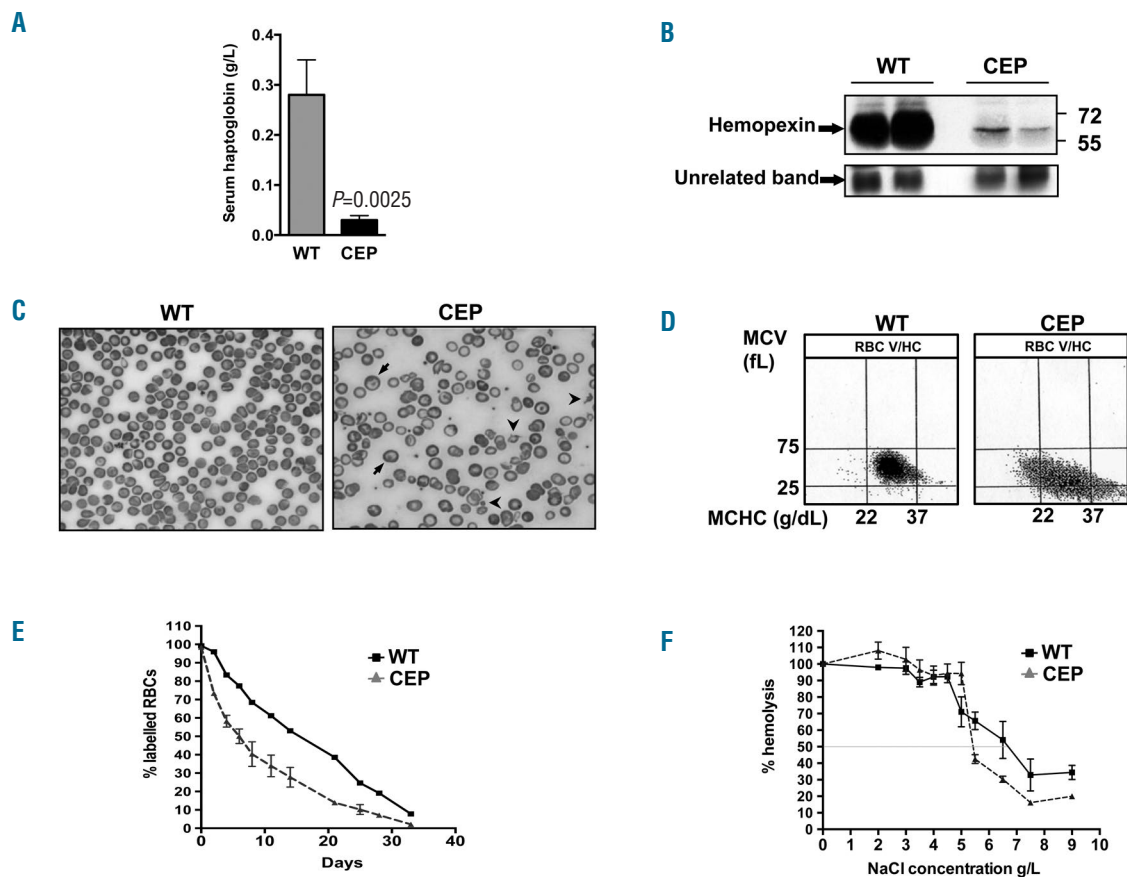
Figure 1. Red blood cell (RBC) morphology, half-life and osmotic fragility in congenital erythropoietic porphyria (CEP) mice. (A) Measurement of serum Hp in controls (WT) and CEP mice. (B) Western blot of plasma Hpx in WT and CEP mice. (Right) Molecular weights in kDa. (C) Red blood cell smears. Anisocytosis and poikilocytosis are shown by arrow heads and hypochromic red cells by arrows. (D) Plot of mean cell Hb concentration (x-axis) against mean cell volume (y-axis) in controls (WT) and CEP mice. Data were obtained with the ADVIA 120 hematology analyzer (Siemens Healthcare Diagnostics, France). One representative mouse is shown for each condition. Similar results were obtained for the other 5 animals. (E) Red blood cell half-life. Biotin was injected on three consecutive days and a small aliquot of blood was analyzed at the indicated times by streptavidin labeling to detect the decay of biotinylated erythrocytes over time. Remaining biotinylated RBCs are expressed as percentage (%) of the total circulating RBCs. Results are the mean±Standard Deviation (SD) of results obtained on n=3 mice for each group. (F) Osmotic fragility of erythrocytes was evaluated in WT (black rectangles) and in CEP (gray triangle) mice. Results are expressed as percentage (%) of hemolysis in distilled water (set to 100%) against the NaCl concentration in the test solution.

(Figure 2A). In addition, the number of late erythroblasts was much lower than the intermediate erythroblasts in CEP mice, suggesting increased maturation rate and cellular exit from the bone marrow. The spleen of CEP animals was grossly enlarged (*Online Supplementary Figure S2B*), as previously reported,[7] resulting from the onset of spleen erythropoiesis. Indeed, in this organ, there was a strong increase in the total number of erythroblasts at all stages of differentiation (Figure 2C). However, in contrast to the bone marrow, there was no significant decrease between intermediate and late erythroblasts (Figure 2C) and we observed decreased rather than increased apoptosis, as usually observed in ineffective erythropoiesis[22,23] (Figure 2D). In adult spleen, stress erythropoiesis may be induced during acute anemia and hypoxia by BMP4 (Bone Morphogenic Protein 4) factor.[24,25] We thus analyzed BMP4 expression level in CEP mice and show its strong increase in the red pulp of the spleen (Figure 2E), likely contributing to the rapid formation of stress burst-forming unit erythroid progenitors (BFU-Es) as a consequence of the high levels of erythropoietin (Epo) in these mice (Table 1).

Therefore, hemolytic anemia in CEP mice activates a compensatory stress erythropoiesis with no sign of ineffective erythropoiesis.

Regenerative anemia represses hepcidin expression

Increased Epo levels and regenerative erythropoiesis are known to repress hepcidin expression. We thus investigated their impact on hepcidin synthesis and iron status in CEP mice. As expected, hepcidin was markedly reduced, both in the liver (at the mRNA level) and in the serum (Figure 3A and B). *Fam132b* mRNA expression in bone marrow cells was significantly increased (30-fold compared to WT mice) (Figure 3C). Using isolated duodenal loops to measure the transepithelial iron transport, we found that CEP mice presented a higher rate of iron absorption than the WT mice, although the differences between the area under the curves did not reach statistical significance (Figure 3D). In addition, we observed an increase of ferroportin protein expression in duodenal enterocytes (Figure 3E and F). Serum iron was also increased in CEP mice, but this did not lead to elevated Tf
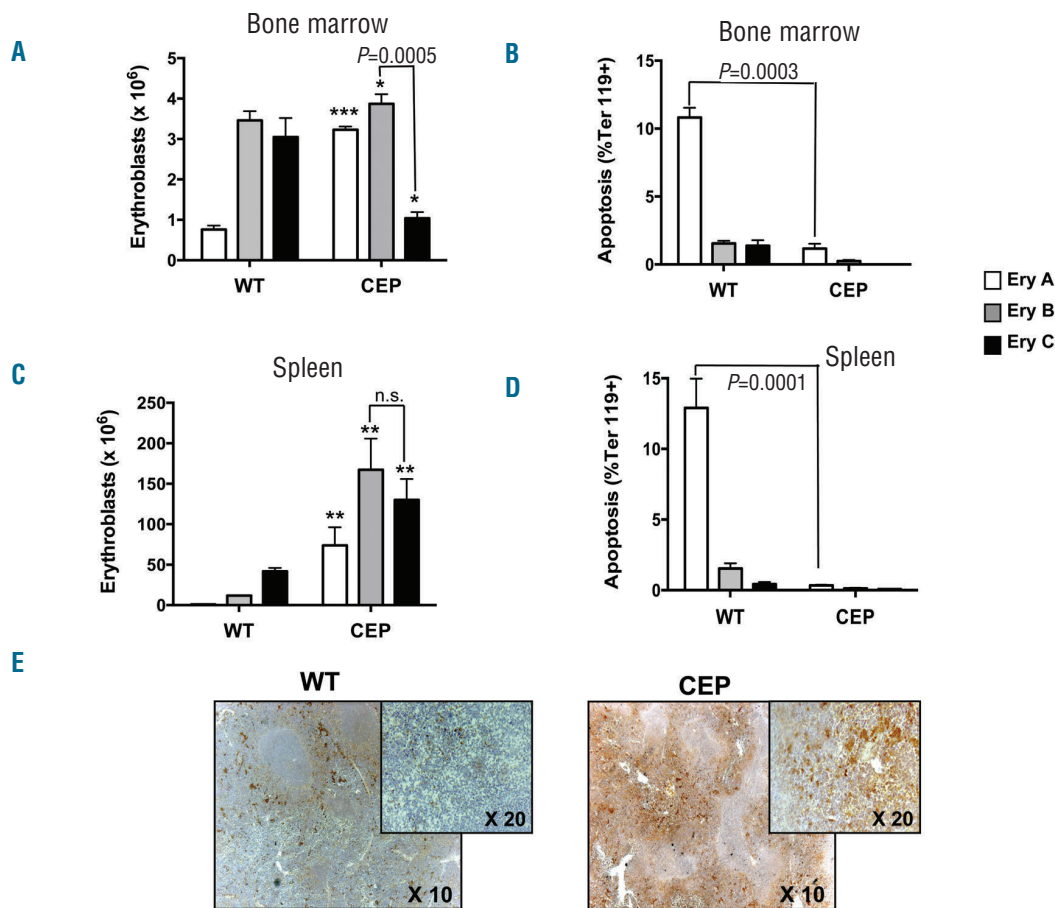
Figure 2. Erythroblast subpopulations in bone marrow and spleen of congenital erythropoietic porphyria (CEP) mice and spleen BMP4 expression. The number of erythroblasts at different stages of maturation (A and C) and the proportion of Annexin V+ cells in each subset of erythroblast (B and D) was analyzed in bone marrow (A and B) and spleen (C and D). The proportion of erythroblasts at each stage of maturation was determined by FACS and the corresponding number of erythroblasts was calculated based on the observation that a femur contains 20x10^{6} cells and a spleen contains 10[6] cells/mg wet weight.[14] The three stages correspond to early (Ery A, white bars), intermediate (Ery B, gray bars), and late erythroblasts and reticulocytes (Ery C, black bars). Results are expressed as mean±Standard Error of the Mean (SEM) obtained for 3 animals of each genotype. The number of erythroblasts differed significantly between WT and CEP mice at all three stages of differentiation in the bone marrow (A) (*P=0.01, **P<0.05, ***P<0.0001; Student *t*-test) and in the spleen (C) (P=0.03). (E) Immunohistochemical staining of BMP4 in the spleen of WT and CEP mice (original magnifications 10x and 20x). n.s.: not significant.

saturation because Tf was also significantly increased, which is reminiscent of iron deficiency anemia and facilitates iron delivery to a larger number of erythroblasts (Table 1 and Figure 3G).

Tissue iron overload is strongly held in macrophages

As expected, serum ferritin was significantly increased in CEP mice (Figure 3H). This increase was associated with higher iron content of the liver (1589±395 µg/g tissue in CEP *vs.* 443±573 µg/g tissue in WT; *P*=0.004). In the spleen, the concentration of iron was only moderately increased in CEP mice (1158±205 µg/g tissue in WT *vs.* 1739±332 µg/g tissue in CEP; *P*=0.004); however, due to a sharp increase in size (*Online Supplementary Figure S2B*), the total amount of iron was grossly increased from 145±35 in WT to 2157±740 g in CEP (*P*<0.0001). Furthermore, Perl's staining in CEP mice shows that heavy iron deposits in the liver were restricted to Kupffer cells while only a diffuse, fainter staining was observed in hepatocytes (Figure 4A). This pattern of iron accumulation differs from the primary hemochromatosis mouse models (including *Hjv*^{–/–} mice)[26-28] where Tf saturation is high[19] and

iron is mostly accumulated in hepatocytes (Figure 4A). Iron was also detected in the macrophages of the red pulp of CEP mice, while almost no iron deposit was observed in the spleen of *Hjv*^{–/–} mice (Figure 4B), confirming that Hb and "free" heme are the likely source of macrophage iron accumulation. Therefore, these data suggest that, in chronic hemolysis, release of Hb in plasma contributes to macrophage iron overload preferentially and that Tf-bound iron that is massively used to meet the high demand of regenerative erythropoiesis in bone marrow and spleen contributes only moderately to tissue iron loading. However, one cannot exclude the possibility that hepatocyte iron overload could appear in older animals.

The Hp plasma concentration was very low in CEP mice (Figure 1A), probably because of an increased rate of its endocytosis and subsequent lysosomal degradation. Interestingly, in both liver and spleen, the expression of the Hb-Hp receptor (CD163)[29] was found to be fully suppressed at both the mRNA and protein levels (Figure 4C and D and *Online Supplementary Figure S1B*), suggesting a slowdown of Hb uptake in macrophages which may prevent excess iron overload. Heme released from Hb is
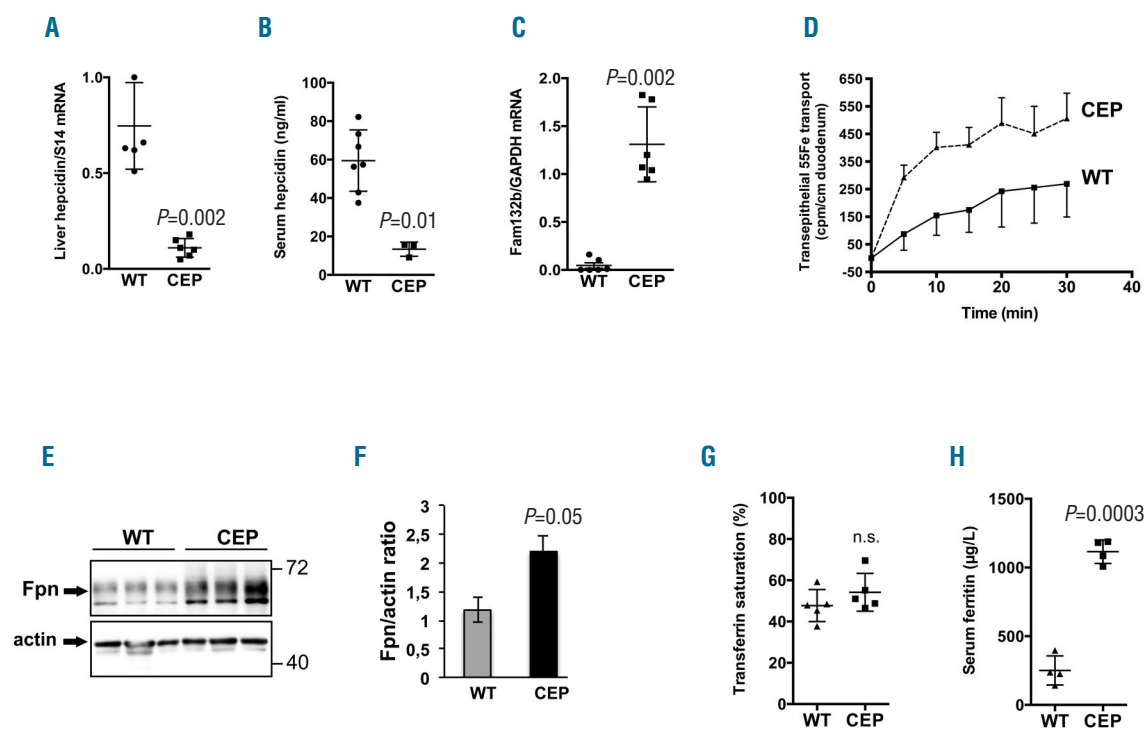
Figure 3. Iron parameters in congenital erythropoietic porphyria (CEP) mice. Wild-type (WT, control) and CEP mice were explored as follows. (A) Quantitative PCR analysis of Hamp1 (hepcidin) mRNA expression in the liver, normalized by S14 mRNA. (B) Serum hepcidin level measured by LC-MS/MS. (C) Quantitative PCR analysis of *Fam132b* mRNA expression in the bone marrow, normalized by *Gapdh* mRNA. (D) Transepithelial iron transport in isolated duodenal loops evaluated as described in the Methods section. (E) Western blot analysis of ferroportin (Fpn) in duodenal enterocytes. β-actin is shown as a loading control. The Fpn antibody is known to give a non-specific 55 KDa band.[14,41] (Left) Molecular weight markers are shown in kDa (F) Quantitative analysis of Fpn protein expression evaluated as ratio to actin abundance. (G) Calculation of transferrin saturation (%) based on the measurement of serum iron and transferrin. (H) Serum ferritin level (μg/L). All results are mean±Standard Error of the Mean (SEM) of at least 4 independent mice. n.s.: not significant.

bound by Hpx and the heme-Hpx complex is mostly taken up by hepatocyte CD91 receptor to be degraded in lysosomes.[30] The mRNA level of CD91 was significantly reduced in the liver and was fully suppressed in the spleen (*Online Supplementary Figure S1A and B*). Thus, like Hb, heme uptake appears to be decreased to protect hepatocytes from iron overload and heme pro-inflammatory effects. Moreover, HO-1 was highly expressed in the liver of CEP compared to WT mice (Figure 4E), confirming that residual heme uptake is rapidly degraded in the liver. In addition, despite an increase in ferritin expression, ferroportin expression was also induced in the liver of CEP mice (Figure 4E), suggesting an increase of iron release in the circulation to satisfy the high iron demand. In the spleen, where the steady state protein levels of HO1 and ferroportin were already high, we observed no difference between control and mutant mice (*Online Supplementary Figure S2A*).

Urinary iron losses contribute to the iron-restricted anemia

Since the CD163 expression was fully suppressed both in liver and spleen, we analyzed Hb excretion in urine. Total urinary iron measured using Inductively Coupled Plasma Optical Emission Spectrometry (ICP-OES) was found at very high levels in CEP mice (from 9.9±5.5 μmol/L in WT to 223.6±113 μmol/L in CEP animals; *P*<0.001) (Figure 5A). The determination of urinary non-heme iron by the method normally used for serum iron gave values of 2.2 μmol/L in WT mice and 56 μmol/L in CEP mice, indicating that approximately 75% of the urinary iron is organic. Indeed, using affinity-purified anti-mouse Hb, the histological analysis of kidney sections confirmed the appearance of significant Hb labeling at the apical membrane of CEP proximal tubules (Figure 5B). Interestingly, in contrast with the preserved mRNA levels (*data not shown*), the immunostaining of the endocytic receptor megalin/cubilin complexes revealed evidence of increased cubilin protein expression (Figure 5B) with no significant changes in megalin protein abundance (*data not shown*). Given that megalin/cubilin receptors are responsible for the uptake of glomerular filtrate proteins by the proximal tubules, we measured proteinuria in both WT and CEP mice. The results showed reduced amount of total urinary proteins and urinary albumin in CEP compared to WT mice (Figure 5C and D), suggesting induced function of the megalin/cubilin endocytic receptor in these mice. The toxicity of Hb on renal function was evaluated by the measurement of both serum urea levels and creatinine clearance calculations, and by the histological examination of kidney sections. We could not detect any evidence of renal injury in the CEP mice compared to WT mice, at least until the age of 14 weeks (Figure 5E and F and *Online Supplementary Figure S3*). Next, we explored the intrinsic heme and iron handling by the kidney in CEP mice. As expected, Perl's staining of CEP kidneys showed significant accumulation of iron in the renal cortical part, particularly in the proximal tubules (Figure 6A). Ferritin
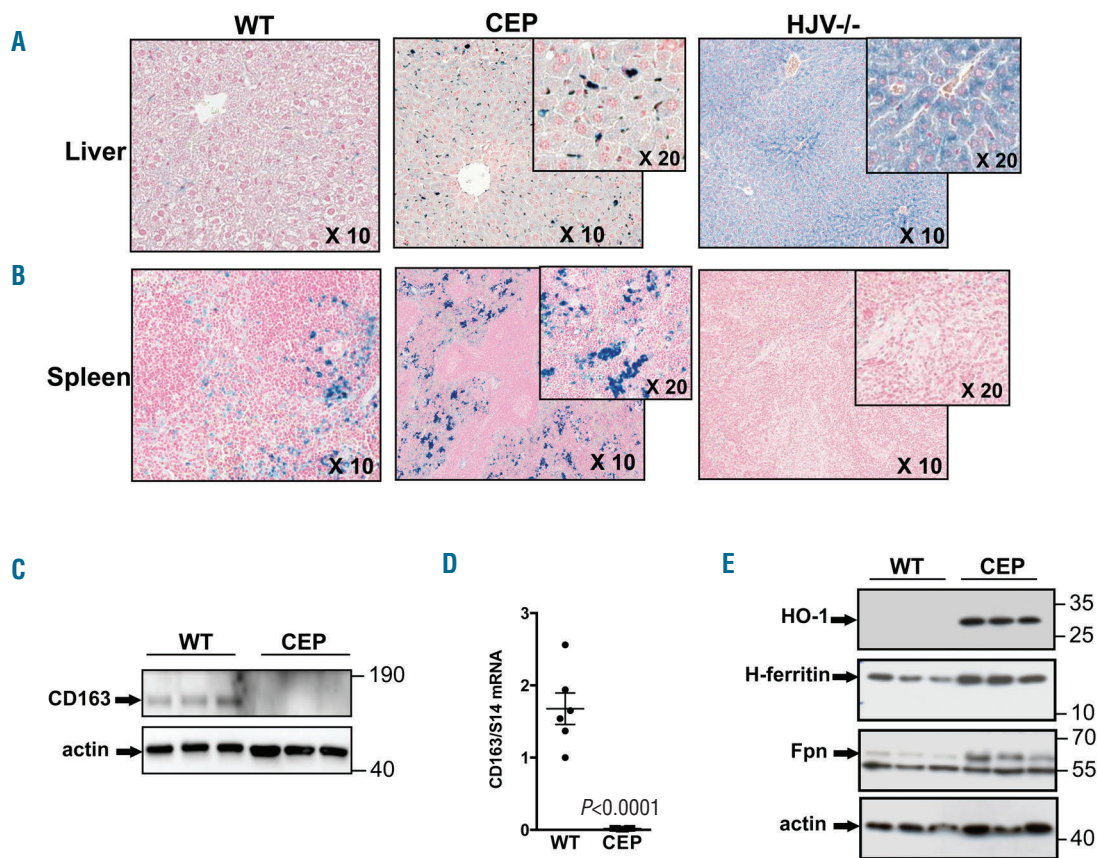
Figure 4. Hemoglobin, heme and iron processing in liver and spleen of congenital erythropoietic porphyria (CEP) mice. Perl's staining of iron loading in the liver (A) and spleen (B) of wild-type (WT, control), CEP and *Hjv*⁻/⁻ mice. In CEP mice, non-heme iron deposits were detected in liver Kupffer cells and in the spleen red pulp macrophages in CEP mice, whereas in *Hjv*⁻/⁻ mice, non-heme iron was accumulated in hepatocytes (magnification 10X and 20X). (C) Western blot of the CD163 in the liver of WT and CEP mice. β-actin is shown as a loading control. (D) Quantitative PCR analysis of CD163 mRNA expression in the liver of WT and CEP mice, normalized by S14 mRNA. Results are mean±Standard Error of the Mean (SEM) of 6 independent mice. (E) Western blot analysis of HO1, H ferritin and ferroportin in the liver of of WT and CEP mice. β-actin is shown as a loading control.

protein level was significantly increased in the cortex but not in the medulla of CEP mice, confirming exclusive iron handing in the proximal renal tubules in these mice (Figure 6B); no change in the mRNA-expression of ferritin was observed (Figure 6B). However, the mRNA and protein expression of both TFR1 and DMT1 responsible for iron entry into renal cells were slightly decreased, although not reaching statistical significance (*Online Supplementary Figure S4*). Interestingly, the mRNA expression levels of HO-1 and ferroportin, which are both induced transcriptionally by free heme, were enhanced significantly in the cortex, but not in the medulla, of CEP mice, resulting in large increases in their protein abundance (Figure 6C). We also measured the portion of free heme in the urine of these mice using a hemin assay kit and found that only small traces of urinary free heme were detectable in WT mice and these were only slightly increased in the urine of CEP mice (0.68±0.2 μmol/L in WT to 6.7±0.2 μmol/L in CEP animals; *P*<0.03). To test whether this portion of heme results from Hb catabolism or from free heme waste, we studied heme and iron metabolism in PHZ-treated mice (used as a model of acute hemolysis) and in mice that were (i.p.)-injected daily with heme arginate (HA) for three weeks. The control mice were injected with excipients. Both increased urinary iron and heme levels and induced cortical HO-1 and ferroportin mRNA levels were observed solely in PHZ-mice but not in non-heme (NH) mice (*Online Supplementary Table S1* and *Figure S5*). In addition, by Perl's staining, iron overload in NH mice was localized primarily in the spleen, and to a lesser extent in the liver, but not in the kidney, indicating that the kidney may contribute to Hb rather than free heme handling in conditions of hemolysis (*Online Supplementary Figure S5*).

Altogether, our results suggest that the kidney, by specifically handling Hb and recovering iron through ferroportin, likely limits deleterious effects of hemolytic anemia in CEP mice.

Discussion

Our CEP mouse model exhibiting induced chronic intravascular hemolysis highlighted new insights into iron disorders related to heme and Hb catabolisms. The phenotype of this iron disorder, although associated with down-regulation of hepcidin expression, differs strongly from the iron-loading anemia that is associated to ineffective erythropoiesis. Indeed, CEP mice mounted an efficient
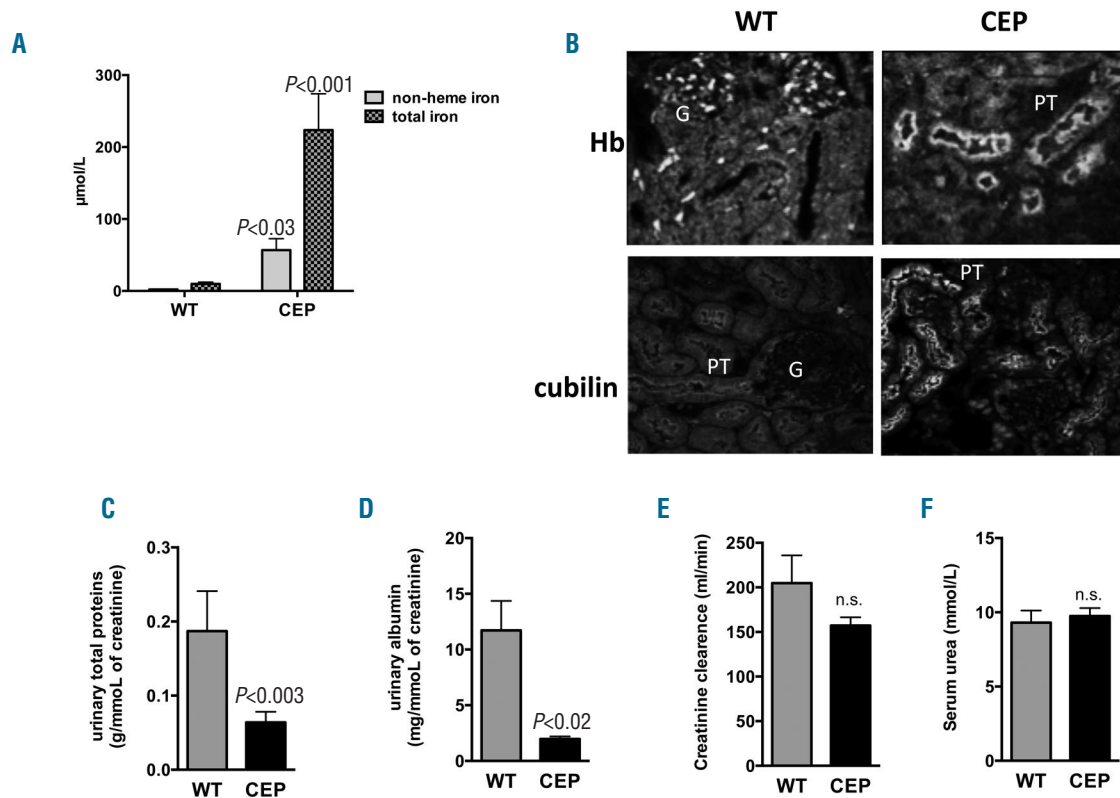
Figure 5. Hb clearance in the kidney of congenital erythropoietic porphyria (CEP) mice. (A) Non-heme iron (gray bars) and total iron (striped bars) was measured in the urine of wild-type (WT, control) and CEP mice. The results are mean±Standard Error of the Mean (SEM) of 6 independent mice. (B) Immunofluorescence staining of hemoglobin (Hb) and cubilin in the kidney of WT and CEP mice. G: glomerous; PT: proximal tubule (original magnifications 40X). (C-F) Urinary total protein, albumin, creatinine clearance and serum urea, respectively, measured in the urine of WT and CEP mice. Results are mean±Standard Error of the Mean (SEM) of 6 independent mice.

erythroid response and normal transferrin saturation, which, together with urinary iron-bound Hb losses, limited excess iron deposition in hepatocytes.

The increased RDW of CEP red cells most likely contributed to hemolysis. The inability of RBCs to control their volume is known to impair their function, including their ability to undergo membrane deformation during circulation in the vasculature.[31] The observed anemia was highly regenerative but was also microcytic, with microcytosis already present at the level of reticulocytes. This finding suggests that heme synthesis was reduced during erythroblast maturation most likely because of reduced protoporphyrin IX (PPIX) synthesis. In addition, the CEP mice showed decreased CHr, a known marker of true iron deficiency.[21,32] Therefore, iron supply to the developing erythroblast could also be a rate-limiting factor in our CEP mice because of both a highly regenerative erythropoiesis and iron losses associated with hemolysis. Indeed, hepcidin expression was reduced and led to increased intestinal iron absorption, as shown by our experiments on isolated duodenal loops. Furthermore, ferroportin, which exports iron from tissues back to the plasma, was highly induced in CEP mice, suggesting that tissue iron stores can be efficiently mobilized. Transferrin saturation is still within the normal range, suggesting that increased intestinal iron absorption and macrophages heme-iron recycling are sufficient to compensate for the urinary iron losses. We also showed that Fam 132b (ERFE), a factor produced by developing erythroblasts and implicated in Hamp gene repression,[3] was highly up-regulated in bone marrow and erythropoietic spleen in conditions of chronic hemolysis and is likely to contribute to hepcidin repression. Furthermore, it has been shown that this erythropoietic signaling pathway can override hepcidin regulation by iron, as shown by the paradoxical association of low serum hepcidin levels and tissue iron overload both in mouse models[22,33,34] and patients[5,35] with β thalassemia, congenital dyserythropoietic anemia,[36] or myelodysplastic syndrome.[4]

The normal Tf saturation seemed to limit iron loading of hepatocytes, on the contrary to what is observed in hemochromatosis with normal erythropoiesis or in iron-loading anemia with ineffective erythropoiesis, where hepcidin is also fully suppressed but leads to heavy hepatocyte iron overload.[22,33,34] In hemolytic conditions, heme- and Hb-derived iron contributes to tissue iron loading independently of Tf-bound iron. Hb makes stable complexes with Hp before being taken up by macrophages through binding and internalization by CD163.[29] Interestingly, Hp was almost undetectable in the plasma of the CEP mice and the CD163 mRNA expression was fully suppressed both in liver and spleen, suggesting that both tissues are able to deploy intrinsic mechanisms to reduce free Hb management, and thus to be protected from its
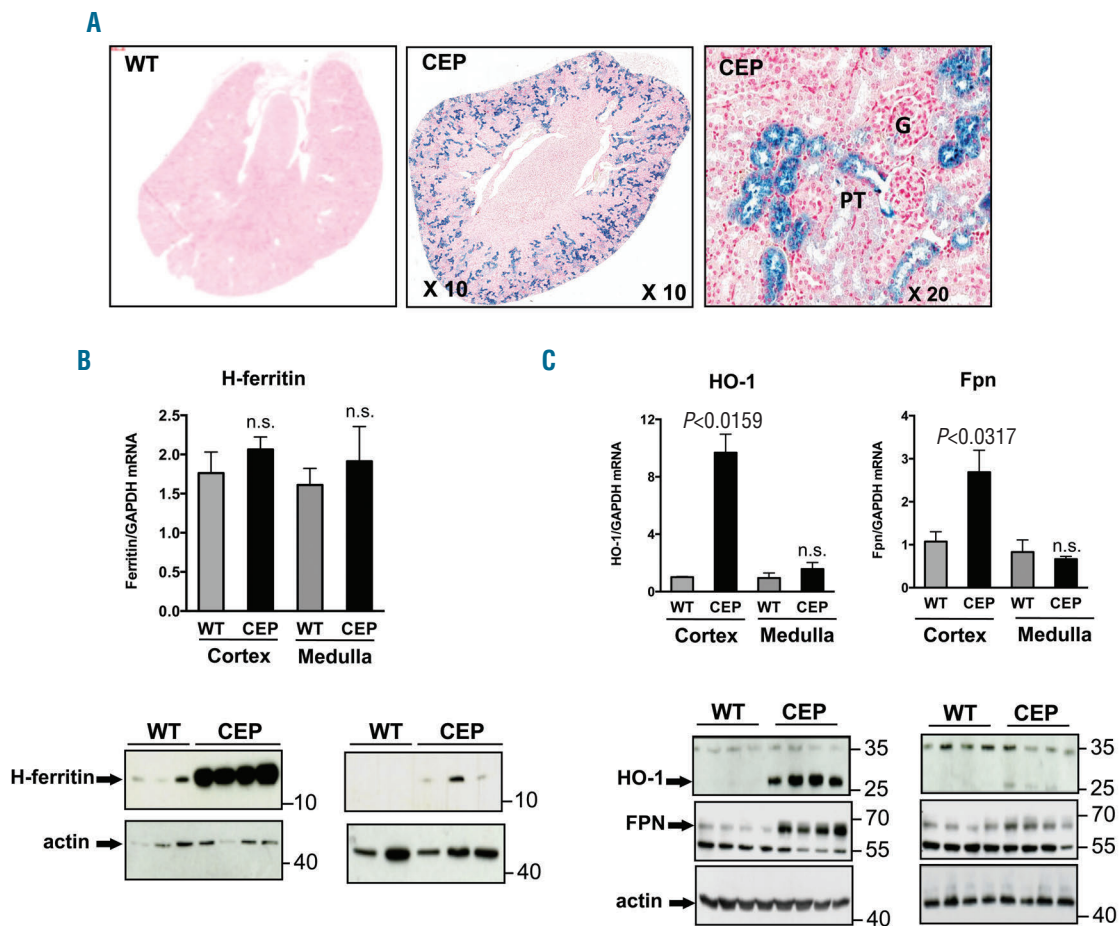
Figure 6. Heme and iron processing in the kidney of congenital erythropoietic porphyria (CEP) mice. (A) Perl's staining of iron loading in the kidney of wild-type (WT, control) and CEP mice. Non-heme iron deposits were detected in the proximal tubules. G: glomerous; PT: proximal tubule (magnification 10x and 20x). (B and C) Quantitative PCR and western-blot analysis of H-ferritin (B), HO1, and Fpn (C) in the cortex and medulla of WT and CEP kidneys. For quantitative PCR analysis, mRNA expression is normalized by actin mRNA. Results are mean±Standard Error of the Mean (SEM) of 6 independent mice. For western blot analysis, β-actin is shown as a loading control. n.s.: not significant.

cytotoxicity. Both free heme and Hb have been shown to down-regulate the mRNA expression of the CD163 in cultures of human monocyte-derived macrophages.[37] In addition, when the buffering capacity of Hp is overwhelmed, Hb is oxidized into methemoglobin which liberates its heme rapidly.[30] Heme is then bound by Hpx and cleared by internalization of the complex by CD91.[38] Expression of this receptor is ubiquitous but the presence of iron deposits in the CEP and HA mice, mostly in macrophages of the spleen and the liver, is indicative of dominant heme uptake by macrophages. Furthermore, Hpx was almost undetectable in the plasma of the CEP mice, suggesting that some heme remained either "free" or loosely bound to albumin and was probably taken up by liver macrophages, as previously demonstrated.[30] Perl's staining of the liver showed that iron accumulated predominantly in macrophages, suggesting that this heme uptake pathway was operative in macrophages, similarly to what was seen in the superoxide dismutase 1 knockout mouse model also characterized by chronic hemolysis, and the animals were analyzed at one year of age.[39]

Our results also highlight the involvement of the kidney in Hb and iron in the context of hemolytic anemia. We

have previously shown that the kidney exhibits a cell specificity of iron handling in the kidney, which depends on the pathological origin of the iron overload. In hemochromatosis models, transferrin-bound iron was specifically handled in the thick ascending limb;[19] however, as shown in our hemolytic model, Hb-bound iron was specifically taken up by the proximal tubule, the endocytic megalin/cubilin complex was stimulated, and HO-1 and ferroportin were induced to generate and return iron to the bloodstream, although the urinary iron-bound Hb losses remained significant and certainly contribute to the hypochromic anemia. The involvement of renal megalin/cubilin receptors for the binding and uptake of Hb has been previously demonstrated by *in vitro* studies and mouse models.[40] In addition, the upregulation of cubilin in the CEP model illustrates the physiological importance of this receptor in the renal clearance of Hb.

Altogether, we show that chronic intravascular hemolysis in CEP mice is associated with an efficient erythroid response in bone marrow and spleen (Figure 7). Microcytic anemia persists despite repression of hepcidin, increased intestinal iron absorption, renal iron recovery, and regenerative erythropoiesis. This hepcidin repression does not
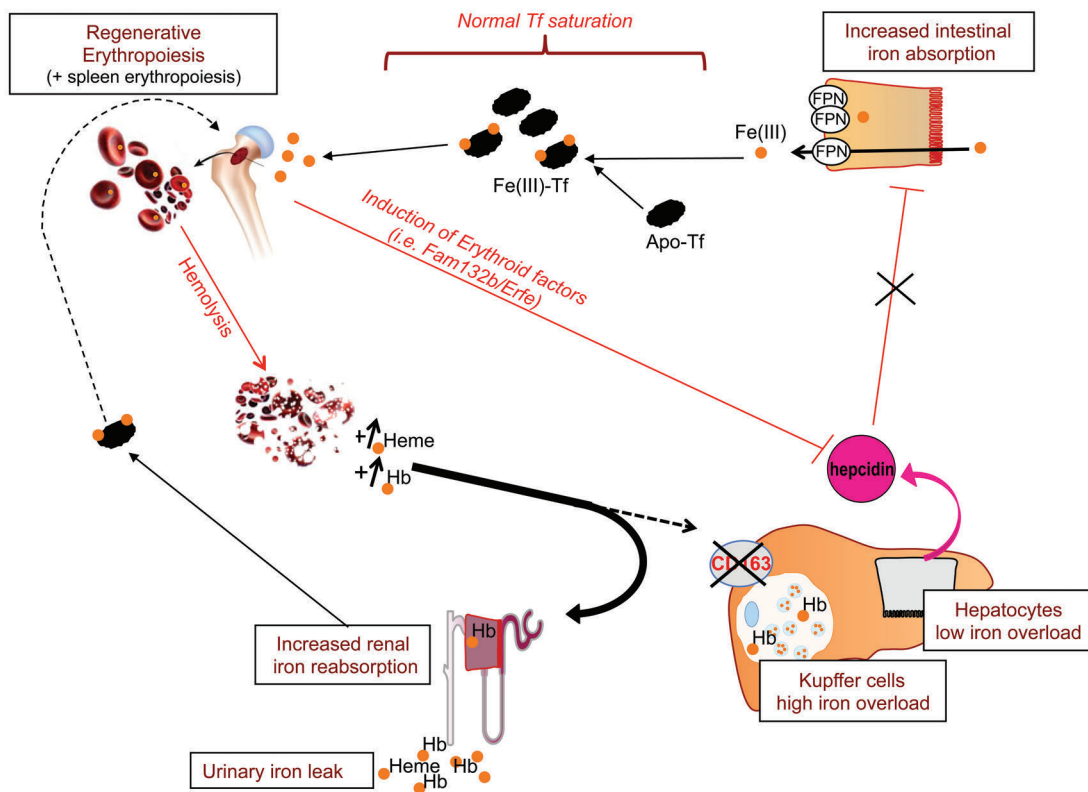
Figure 7. Schematic representation of iron balance in congenital erythropoietic porphyria (CEP) mice. Regenerative anemia associated with hemolysis represses hepcidin expression, thereby increasing intestinal iron absorption and allowing iron recycling by macrophages. Transferrin (Tf) is increased to favor iron delivery to developing erythroblasts and Tf saturation remains normal. Plasma heme and hemoglobin (Hb) contribute to macrophage iron overload, mostly in the liver. However, the reduction of CD163 expression should prevent the uptake of free Hb in the liver, but favor its wasting in the urine. Kidney recovers part of this Hb to recycle iron into the circulation. Combined with urinary Hb-iron losses, normal Tf saturation prevents hepatocyte iron overload.

lead to a significant hepatocyte iron overload. Genes such as CD163 and CD91, involved in iron redistribution following hemolysis, could play a role as a modifier of disease severity in human CEP patients as well as in other chronic hemolytic disorders. Moreover, our results highlight the crucial involvement of kidney in eliminating the extra toxic Hb and in the recovery of iron to satisfy iron demand for regenerative purposes in the context of hemolytic anemia.

References

1. Ganz T. Hepcidin and iron regulation, 10 years later. Blood. 2011;117(17):4425-4433.
2. De Falco L, Silvestri L, Kannengiesser C, et al. Functional and clinical impact of novel TMPRSS6 variants in iron-refractory iron-deficiency anemia patients and genotype-phenotype studies. Hum Mutat. 2014;35(11):1321-1329.
3. Kautz L, Jung G, Valore EV, et al. Identification of erythroferrone as an erythroid regulator of iron metabolism. Nat Genet. 2014;46(7):678-684.
4. Santini V, Girelli D, Sanna A, et al. Hepcidin levels and their determinants in different types of myelodysplastic syndromes. PLoS One. 2012;6(8):e23109.
5. Tanno T, Bhanu NV, Oneal PA, et al. High levels of GDF15 in thalassemia suppress expression of the iron regulatory protein hepcidin. Nat Med. 2007;13(9):1096-1101.
6. Nielsen MJ, Moller HJ, Moestrup SK. Hemoglobin and heme scavenger receptors. Antioxid Redox Signal. 2009;12(2):261-273.
7. Ged C, Mendez M, Robert E, et al. A knock-in mouse model of congenital erythropoietic porphyria. Genomics. 2006;87(1):84-92.
8. Ged C, Moreau-Gaudry F, Richard E, Robert-Richard E, de Verneuil H. Congenital erythropoietic porphyria: mutation update and correlations between genotype and phenotype. Cell Mol Biol (Noisy-le-grand). 2009;55(1):53-60.

9. Puy H, Gouya L, Deybach JC. Porphyrias. Lancet. 2011;375(9718):924-937.

10. Katugampola RP, Anstey AV, Finlay AY, et al. A management algorithm for congenital erythropoietic porphyria derived from a study of 29 cases. Br J Dermatol. 2012;167(4):888-900.

11. To-Figueras J, Ducamp S, Clayton J, et al. ALAS2 acts as a modifier gene in patients with congenital erythropoietic porphyria. Blood. 2011;118(6):1443-1451.

12. Robert-Richard E, Moreau-Gaudry F, Lalanne M, et al. Effective gene therapy of mice with congenital erythropoietic porphyria is facilitated by a survival advantage of corrected erythroid cells. Am J Hum Genet. 2008;82(1):113-124.

13. Latour C, Kautz L, Besson-Fournier C, et al. Testosterone perturbs systemic iron balance through activation of epidermal growth factor receptor signaling in the liver and repression of hepcidin. Hepatology. 2014;59(2):683-94.

14. Millot S, Andrieu V, Letteron P, et al. Erythropoietin stimulates spleen BMP4-dependent stress erythropoiesis and partially corrects anemia in a mouse model of generalized inflammation. Blood. 2011; 116(26):6072-6081.

15. Brasse-Lagnel C, Karim Z, Letteron P, Bekri S, Bado A, Beaumont C. Intestinal DMT1 cotransporter is down-regulated by hepcidin via proteasome internalization and degradation. Gastroenterology. 2011; 140(4):1261-1271 e1.

16. Lockwood WH, Poulos V, Rossi E, Curnow DH. Rapid procedure for fecal porphyrin assay. Clin Chem. 1985;31(7):1163-1167.

17. Lim CK, Peters TJ. Urine and faecal porphyrin profiles by reversed-phase high-performance liquid chromatography in the porphyrias. Clin Chim Acta. 1984; 139(1):55-63.

18. Delaby C, Pilard N, Goncalves AS, Beaumont C, Canonne-Hergaux F. Presence of the iron exporter ferroportin at the plasma membrane of macrophages is enhanced by iron loading and down-regulated by hepcidin. Blood. 2005;106(12):3979-3984.

19. Moulouel B, Houamel D, Delaby C, et al. Hepcidin regulates intrarenal iron handling at the distal nephron. Kidney Int. 2013; 84(4):756-766.

20. Lyoumi S, Abitbol M, Andrieu V, et al. Increased plasma transferrin, altered body iron distribution, and microcytic hypochromic anemia in ferrochelatase-deficient mice. Blood. 2007;109(2):811-818.

21. Brugnara C, Laufer MR, Friedman AJ, Bridges K, Platt O. Reticulocyte hemoglobin content (CHr): early indicator of iron deficiency and response to therapy. Blood. 1994;83(10):3100-3101.

22. De Franceschi L, Daraio F, Filippini A, et al. Liver expression of hepcidin and other iron genes in two mouse models of beta-thalassemia. Haematologica. 2006; 91(10):1336-1342.

23. Li R, Rybicki AC, Suzuka SM, et al. Transferrin therapy ameliorates disease in beta-thalassemic mice. Nat Med. 2010; 16(2):177-182.

24. Perry JM, Harandi OF, Paulson RF. BMP4, SCF, and hypoxia cooperatively regulate the expansion of murine stress erythroid progenitors. Blood. 2007;109(10):4494-4502.

25. Paulson RF, Shi L, Wu DC. Stress erythropoiesis: new signals and new stress progenitor cells. Curr Opin Hematol. 2011;18(3): 139-145.

26. Huang FW, Pinkus JL, Pinkus GS, Fleming MD, Andrews NC. A mouse model of juvenile hemochromatosis. J Clin Invest. 2005; 115(8):2187-2191.

27. Meynard D, Kautz L, Darnaud V, et al. Lack of the bone morphogenetic protein BMP6 induces massive iron overload. Nat Genet. 2009;41(4):478-481.

28. Nicolas G, Bennoun M, Devaux I, et al. Lack of hepcidin gene expression and severe tissue iron overload in upstream stimulatory factor 2 (USF2) knockout mice. Proc Natl Acad Sci USA. 2001;98(15):8780-8785.

29. Kristiansen M, Graversen JH, Jacobsen C, et al. Identification of the haemoglobin scavenger receptor. Nature. 2001; 409(6817): 198-201.

30. Tolosano E, Fagoonee S, Morello N, Vinchi F, Fiorito V. Heme scavenging and the other facets of hemopexin. Antioxid Redox Signal. 2011;12(2):305-320.

31. An X, Mohandas N. Disorders of red cell membrane. Br J Haematol. 2008;141(3): 367-375.

32. Brugnara C. Reticulocyte cellular indices: a new approach in the diagnosis of anemias and monitoring of erythropoietic function. Crit Rev Clin Lab Sci. 2000;37(2):93-130.

33. Gardenghi S, Marongiu MF, Ramos P, et al. Ineffective erythropoiesis in beta-thalassemia is characterized by increased iron absorption mediated by down-regulation of hepcidin and up-regulation of ferroportin. Blood. 2007;109(11):5027-5035.

34. Ramos P, Melchiori L, Gardenghi S, et al. Iron metabolism and ineffective erythropoiesis in beta-thalassemia mouse models. Ann N Y Acad Sci. 2010;1202:24-30.

35. Origa R, Galanello R, Ganz T, et al. Liver iron concentrations and urinary hepcidin in beta-thalassemia. Haematologica. 2007; 92(5):583-588.

36. Tamary H, Shalev H, Perez-Avraham G, et al. Elevated growth differentiation factor 15 expression in patients with congenital dyserythropoietic anemia type I. Blood. 2008;112(13):5241-5244.

37. Schaer CA, Vallelian F, Imhof A, Schoedon G, Schaer DJ. Heme carrier protein (HCP-1) spatially interacts with the CD163 hemoglobin uptake pathway and is a target of inflammatory macrophage activation. J Leukoc Biol. 2008;83(2):325-333.

38. Hvidberg V, Maniecki MB, Jacobsen C, et al. Identification of the receptor scavenging hemopexin-heme complexes. Blood. 2005; 106(7):2572-2579.

39. Starzynski RR, Canonne-Hergaux F, Willemetz A, et al. Haemolytic anaemia and alterations in hepatic iron metabolism in aged mice lacking Cu,Zn-superoxide dismutase. Biochem J. 2009;420(3):383-390.

40. Gburek J, Verroust PJ, Willnow TE, et al. Megalin and cubilin are endocytic receptors involved in renal clearance of hemoglobin. J Am Soc Nephrol. 2002;13(2):423-430.

41. Lasocki S, Millot S, Andrieu V, et al. Phlebotomies or erythropoietin injections allow mobilization of iron stores in a mouse model mimicking intensive care anemia. Crit Care Med. 2008;36(8):2388-2394.